Fusion Engineering and Design xxx (2017) xxx–xxx

Contents lists available at ScienceDirect

Fusion Engineering and Design

journal homepage: www.elsevier.com/locate/fusengdes

Traditional vs. advanced Bragg reflectors for oversized circular waveguide

S. Ceccuzzi[a,*], A. Doria[a], G.P. Gallerano[a], G.L. Ravera[a], I. Spassovsky[a], N.S. Ginzburg[b], M. Yu. Glyavin[b], N. Yu. Peskov[b], A.V. Savilov[b]

[a] ENEA, Fusion Physics Division, Via E. Fermi 45, 00044 Frascati (Rome), Italy
[b] Institute of Applied Physics RAS, Nizhny Novgorod, Russia

HIGHLIGHTS

- A mode-matching code is applied to electrically large Bragg reflectors.
- Traditional and advanced distributed reflectors are compared.
- The traditional mirror has larger bandwidth and lower ohmic losses.
- The advanced mirror is shorter.

ARTICLE INFO

Article history:
Received 3 October 2016
Received in revised form 21 January 2017
Accepted 15 February 2017
Available online xxx

Keywords:
Distributed Bragg reflector
CARM
Oversized waveguide
Corrugated waveguide

ABSTRACT

This paper compares two types of distributed Bragg reflector, based on the periodic wall perturbation of an oversized circular waveguide. The first type is a traditional mirror, where wall ripples with a period of half a guided wavelength for the working mode couple forward and backward waves. The other type is an advanced reflector with a ripple period of about a guided wavelength, exploiting an intermediate conversion into a quasi-cutoff mode. The design of both reflectors has been optimized with a mode matching code to deliver a reflectivity >96% for the $TE_{5,3}$ mode at 250 GHz and a power to gun <0.5% in copper waveguides with a diameter of 15 mm. Such specifications are relevant to the upstream mirror of a cyclotron auto-resonance maser under development at ENEA Frascati. The two types of reflector are compared in terms of mechanical dimensions, reflectivity, bandwidth and losses.

1. Introduction

Cyclotron auto-resonance masers (CARMs) are vacuum electron devices based on physical mechanisms that are very promising to achieve efficient continuous-wave (CW) high-power (≥1 MW) high-frequency (≥200 GHz) electromagnetic sources [1], as required for instance by heating & current drive or diagnostic systems for reactor-relevant fusion machines like DEMO [2]. Nowadays, no mm-wave source meets DEMO requirements and CARMs are a potentially attractive solution, to be pursued on a longer term than (and in parallel to) the more mature gyrotrons [3]. Some obstacles against CARM success have been removed during last decades thanks to technological advancements in the development of high-quality electron beams and high-voltage power supplies as well as enhancements in modelling and numerical capabilities. The feasibility study of a 250 GHz CARM with an output power of 100 kW for pulses up to 50 μs has been recently undertaken at ENEA [4] as the first step of a more ambitious project, aimed at achieving a CW 1 MW mm-wave source.

One of the most critical parts of a CARM oscillator is the cavity, which consists of an oversized smooth-wall circular waveguide sandwiched between two rippled-wall sections, as shown in Fig. 1. The one at the gun side, i.e., the upstream mirror, is the most challenging because very high reflectivity is required for a mode far from its cutoff frequency. Here traditional [1] and advanced [5] Bragg reflectors are compared using the upstream mirror of the ENEA CARM as study case. After optimization, their designs are assessed in terms of reflectivity, bandwidth, number of ripples and conductor losses to identify strengths and weaknesses.

* Corresponding author.
E-mail address: silvio.ceccuzzi@enea.it (S. Ceccuzzi).

http://dx.doi.org/10.1016/j.fusengdes.2017.02.059
0920-3796/

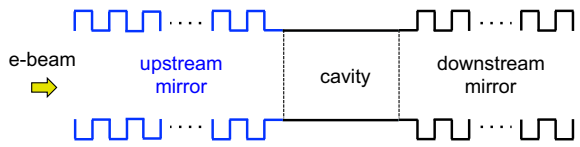

Fig. 1. Sketch of a CARM cavity.

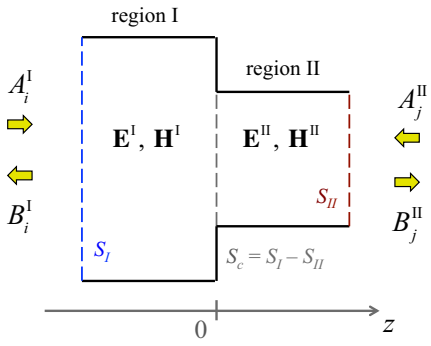

Fig. 2. Step discontinuity.

With respect to [6], this study considers a much more oversized structure, whose working mode is the $TE_{5,3}$, and takes into account ohmic losses. The diameter of ENEA CARM mirrors is around 15 mm, entailing almost 400 propagating modes at 250 GHz and ruling out the use of commercial softwares adopted in [6]. Distributed mirrors have been also addressed by means of coupled mode theory [1,7,8] and mode matching method [8]. The former is an approximate method with some limitations in addressing novel mirror types, so a mode matching code has been specifically developed for this study.

The paper is organized as follows: Section 2 provides a brief description of the numerical method and loss computation. Section 3 describes the reflectors to be assessed, their behaviour and optimization, while in Section 4 their designs are compared. Conclusions are drawn in Section 5.

2. Numerical model

We refer to the step discontinuity of Fig. 2 between circular cross-sections with different diameter. The electromagnetic field, in each section $s = I, II$, is expressed as a modal expansion with unknown amplitudes A and B:

$$\begin{aligned}\mathbf{E}^s &= \sum_{i=1}^{N_s}(A_i^s + B_i^s)\mathbf{e}_{\mathbf{t}_i}^s + (A_i^s - B_i^s)\mathbf{e}_{\mathbf{z}_i}^s \\ \mathbf{H}^s &= \sum_{i=1}^{N_s}(A_i^s - B_i^s)\mathbf{h}_{\mathbf{t}_i}^s + (A_i^s + B_i^s)\mathbf{h}_{\mathbf{z}_i}^s\end{aligned} \tag{1}$$

where subscripts t and z identify transversal and longitudinal components, normalized as in [9]. Actual modal expansions are infinite series, but they have been truncated to a finite number of modes N_s, ordered with increasing cutoff frequency, to allow numerical implementation.

According to Maxwell equations, the total electric and magnetic fields in the two sections must be continuous at the discontinuity plane. The following boundary conditions are obtained in $z = 0$:

$$\mathbf{H}_{\mathbf{t}}^I = \mathbf{H}_{\mathbf{t}}^{II}, \quad \mathbf{E}_{\mathbf{t}}^I = \begin{cases} -Z_w \mathbf{H}_{\mathbf{t}}^I & \text{in } S_c \\ \mathbf{E}_{\mathbf{t}}^{II} & \text{in } S_{II} \end{cases} \tag{2}$$

where the Leontovich condition has been used introducing the surface impedance

$$Z_w = (1+j)\sqrt{\frac{\omega\mu}{2\sigma}} \tag{3}$$

for a metallic wall with magnetic permeability μ and electrical conductivity σ.

The two conditions in (2) are imposed using the Galerkin method: the first one is tested with the generic eigenfunction $\mathbf{h}_{\mathbf{t}_i}^I$, the latter with $\mathbf{e}_{\mathbf{t}_i}^{II}$. Both are integrated over S_I and, after using (1), the following inner products can be defined:

$$\begin{aligned} X_{mn} &= \iint_{S_{II}} \mathbf{e}_{\mathbf{t}_m}^I \times \mathbf{h}_{\mathbf{t}_n}^{II} \cdot \hat{z} dS \\ L_{mn} &= Z_c \iint_{S_c} \mathbf{h}_{\mathbf{t}_m}^I \cdot \mathbf{h}_{\mathbf{t}_n}^I dS \end{aligned} \tag{4}$$

A linear system for the wave amplitudes with $N_I + N_{II}$ equations is obtained:

$$\begin{aligned} \left(\mathbf{A}^I + \mathbf{B}^I\right) &= \mathbf{X}^T \cdot \left(\mathbf{A}^{II} + \mathbf{B}^{II}\right) + \mathbf{L} \cdot \left(\mathbf{A}^I - \mathbf{B}^I\right) \\ \mathbf{X} \cdot \left(\mathbf{A}^I - \mathbf{B}^I\right) &= -\left(\mathbf{A}^{II} + \mathbf{B}^{II}\right) \end{aligned}$$

From this system, the scattering matrix of a single step is readily derived as follows

$$\begin{bmatrix} \mathbf{B}^I \\ \mathbf{B}^{II} \end{bmatrix} = \begin{bmatrix} \mathbf{I}^I - \mathbf{F} & \mathbf{F} \cdot \mathbf{X}^T \\ \mathbf{X} \cdot \mathbf{F} & \mathbf{I}^{II} - \mathbf{X} \cdot \mathbf{F} \cdot \mathbf{X}^T \end{bmatrix} \begin{bmatrix} \mathbf{A}^I \\ \mathbf{A}^{II} \end{bmatrix}$$

where $\mathbf{F} = 2(\mathbf{I}^{II} + \mathbf{X}^T \cdot \mathbf{X} + \mathbf{L})^{-1}$ and $\mathbf{I}^s$ are identity matrices with dimension N_s. Multiple steps are combined through cascading techniques to find the total scattering matrix $\mathbf{S}$ of a reflector. Given the ℓth excitation mode, the fraction of power dissipation due to ohmic losses is

$$1 - \sum_{i=1}^{N_I+N_{II}} \left|S_{i\ell}\right|^2 \tag{5}$$

which delivers approximate results since the attenuation of each mode is calculated separately in segments with constant cross-section and then added.

Critical parameters in the method are the truncation orders N_s of the summations in (1). According to convergence studies [10], an accuracy of about 0.02 on the scattering parameters can be attained by taking into account all modes with cutoff frequency smaller than four times the operational frequency. For the present geometry, this choice corresponds to a huge amount of modes that cannot be handled with ordinary workstations. Nevertheless we are only interested in a column of the scattering matrix, namely when the working mode excites the device, so modes having zero coupling with this mode can be neglected, making the computational load acceptable.

3. Benchmark setup

Traditional and advanced distributed mirrors are based on rippled-wall waveguide with ripple period of $\lambda_g/2$ and λ_g, respectively, being λ_g the wavelength of a guided mode. In the former, the sole forward and backward waves of such mode experience significant coupling, whereas in the latter a three-wave coupling occurs, as sketched in Fig. 3. More precisely, in advanced reflectors, the forward wave is firstly coupled to a mode that operates very close to its cutoff frequency, and transfers its energy back to the reflected wave of the input mode.

In our study case, the circular waveguide has a minimum diameter of 15 mm, step corrugations and copper ($\sigma = 29$ MS/m taking into account surface roughness) as wall material. Each mirror end has 40 (traditional) or 10 (advanced) ripples with tapered depth

Please cite this article in press as: S. Ceccuzzi, et al., Traditional vs. advanced Bragg reflectors for oversized circular waveguide, Fusion Eng. Des. (2017), http://dx.doi.org/10.1016/j.fusengdes.2017.02.059